

Impurity and doping effects on the pseudoenergy gap in CeNiSn: A Sn NMR study

Ko-ichi Nakamura, Yoshio Kitaoka, and Kunisuke Asayama

Department of Material Physics, Faculty of Engineering Science, Osaka University, Toyonaka, Osaka 560, Japan

Toshiro Takabatake

Faculty of Integrated Arts and Sciences and Faculty of Science, Hiroshima University, Higashi-Hiroshima 739, Japan

Go Nakamoto, Hiroaki Tanaka, and Hironobu Fujii

Faculty of Integrated Arts and Sciences, Hiroshima University, Higashi-Hiroshima 739, Japan

(Received 14 August 1995; revised manuscript received 11 October 1995)

Measurements of ^{119}Sn nuclear spin-lattice relaxation rate, $1/T_1$, and Knight shift, K , in the off-stoichiometric compound $\text{CeNi}_{1.01}\text{Sn}$ and the substituted compounds $\text{CeNi}_{1-x}\text{M}_x\text{Sn}$ ($M=\text{Cu,Co}$) and $\text{Ce}_{1-x}\text{La}_x\text{NiSn}$ have been made in order to unravel the impurity and/or carrier doping effects on the V-shaped gapped state in CeNiSn. From the detailed analysis of the T dependence of $1/T_1$, it is shown that the density of states (DOS) is induced just at the Fermi level for $\text{CeNi}_{1.01}\text{Sn}$, whereas the DOS increases progressively with the dopant in a finite-energy range near the Fermi level for the substituted compounds. The respective substitution of Co and La into Ni and Ce sites changes the gapped state into the nonmagnetic Fermi-liquid state, whereas the replacement of Ni by Cu with $x > 0.06$ gives rise to the antiferromagnetic (AF) ground state. It is suggested that the AF order is realized by the combined effect of the rapid collapse of the V-shaped gap and the increase of the DOS at the Fermi level. It has been found to lead to the magnetic ground state and the nonmagnetic Fermi-liquid state to dope electrons and holes into the renormalized conduction bands, respectively.

I. INTRODUCTION

The gapped state is one of the ground states in heavy-electron systems. In such compounds as SmB_6 ($\Delta/k_B \sim 50$ K),¹ YbB_{12} (~ 70 K),² gold SmS (~ 80 K),³ TmSe (~ 30 K),⁴ the presence of an activated energy gap was shown from the transport and the thermal measurements. The gap in these compounds was generally argued to be formed by the hybridization between $4f$ and conduction electrons, whereas the inelastic neutron scattering experiment on SmB_6 suggested that the gap was associated with the local bound state between $4f$ holes and $5d$ electrons with an excitation energy of 14 meV.⁵ A picture that the gap is induced by the hybridization has come into question at the present.

On the other hand, Ce-based compounds such as CeNiSn (Ref. 6), CeRhSb (Ref. 7), and $\text{Ce}_3\text{Bi}_4\text{Pt}_3$ (Ref. 8) have been reported to possess a novel energy gap as well. The gap of $\text{Ce}_3\text{Bi}_4\text{Pt}_3$ is an activated one with the same order of magnitude (~ 70 K) as in the compounds reported so far, whereas it has been argued from various measurements of the magnetic susceptibility, the resistivity, and the thermopower on single-crystal CeNiSn and CeRhSb that a small gap opens in the quasiparticle band with the magnitude of several kelvin that is by one order of magnitude less than the activated gap of the compounds mentioned above. A new type of gapped state in CeNiSn and CeRhSb, named Kondo semiconductors, has attracted much interest.

In contrast to previous results on the resistivity which indicated a significant increase at low T , the T dependence of the resistivity for single-crystal CeNiSn, which was carefully prepared and confirmed to have a better quality than before, has not exhibited a semiconducting behavior along

any crystal direction, but, instead, a metallic behavior.⁹ From this result, it has been suggested that impurities and/or imperfections present in less pure crystals are responsible for an increase of the resistivity at low T , making residual small carriers localized. In this sense, CeNiSn should not be classified as a semiconductor but as a semimetal with a small carrier density.

On the other hand, it is remarkable that the T dependence of $1/T_1$ in CeNiSn and CeRhSb, which decreased largely over *three orders* of magnitude below 10 K, provided firm evidence that the gap opens in the spin excitation spectrum at least. Furthermore, the observation of the $T_1 T = \text{const}$ behavior at very low T for both compounds has also demonstrated the presence of a residual density of states (DOS) at the Fermi level.^{10,11} A prominent outcome from the NMR experiment was thus that the overall T dependence of $1/T_1$ for both compounds was consistently explained by the pseudoenergy-gap model with a V-shaped structure and a small DOS at the Fermi level [see Fig. 1(b)].^{10,11} A motivation to apply such V-shaped structure of the energy gap came from the observation that a decreasing rate of $1/T_1$ seemingly followed a T^3 law at low T . Contrary to this, an exponential decrease of $1/T_1$ probed by ^{209}Bi NMR in $\text{Ce}_3\text{Bi}_4\text{Pt}_3$ was consistent with an *isotropic* energy gap model ($\Delta \sim 180$ K).¹² Thus it is clear that the nature of the gapped state is quite different between CeNiSn and $\text{Ce}_3\text{Bi}_4\text{Pt}_3$ from the NMR experimental point of view.

Furthermore, the spin correlation of CeNiSn was studied by inelastic neutron scattering, which showed that two inelastic peaks developed below around $T=20$ K at $\hbar\omega=4$ and 2 meV at $\mathbf{Q}=(Q_a, 1/2, Q_c)$ and $(0, 0, 1)$, respectively.^{13,14} The \mathbf{Q} dependence of the magnetic excitation at 4 meV was

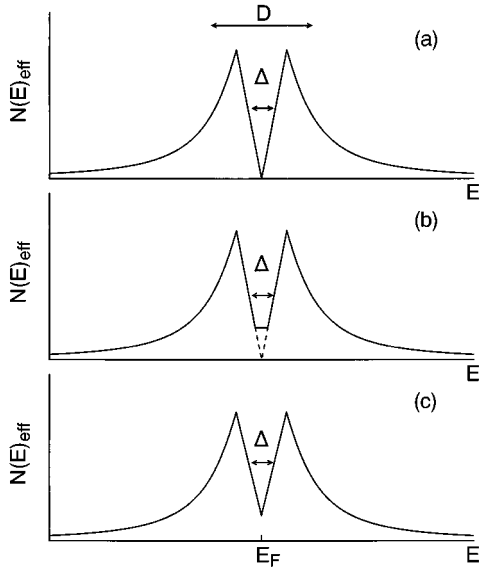


FIG. 1. (a) V-shaped density of states (DOS) for the gapped state in the quasiparticle band of Lorentzian shape proposed previously Ref. 10. (b) Modified V-shaped DOS where the flat DOS is added near the Fermi level to explain $T_1 T = \text{const}$ behavior at low T Ref. 11. (c) Intrinsic “gapless” V-shaped DOS, which possesses a finite DOS at the Fermi level to explain an enhancement of $1/T_1$ of $\text{CeNi}_{1.01}\text{Sn}$ below 1 K.

indicative of the dynamical antiferromagnetic (AF) correlation with a quasi-one-dimensional character along the b axis. The pseudo-spin-gap behavior probed by the NMR measurement is, however, not evident from the neutron scattering experiment.¹⁴

As a result, the gapped state, especially in CeNiSn , is not concluded yet from the transport, the thermal, and the neutron scattering measurements, whereas the pseudo-spin-gap behavior is clear from the T_1 measurement, which identified the V-shaped structure of the gap commonly for both CeNiSn and CeRhSb .^{10,11} In spite of the recent extensive efforts of improving the sample quality of CeNiSn , the NMR and the specific heat results have pointed to the presence of a residual DOS, although the fractions of the DOS is not quantitatively consistent with one another. In this context, CeNiSn and CeRhSb may not be classified as semiconductors but rather semimetals with very low carrier density, i.e., Kondo semimetals in which the spin and the charge response functions possess different energy scales due to the strong electron correlation.

Several models have been proposed to explain the origin of the Kondo insulator thus far. Based on the periodic Anderson model, the Kondo semiconductor or insulator is generally argued as a filling of the Brillouin zone for the quasiparticle band resulting from the weak hybridization or the Kondo-like interaction between localized f and conduction electrons. Extensive studies have reported such effects that (1) the addition of Kondo holes by replacing Ce by La destroys the coherence of the ground state of Kondo insulators and introduces the bound state in the gapped state, (2) Kondo holes with a finite concentration form an impurity band, and (3) to dope carrier and the presence of ligand defects introduce the impurity band in the gap.¹⁵ Importantly, it was

pointed out that the effect of impurity scattering easily gives rise to a finite DOS in the gap, because the treatment in terms of the unitarity limit is generic to the strongly correlated systems, even though the impurity potential is not always strong enough. Apart from a general argument on the Kondo insulator in terms of the periodic Anderson model in which the gap should be of activated type, some theoretical models to explain the unique V-shaped gapped state in CeNiSn and CeRhSb have been put forth so far. The point is that an absence of the hybridization along a certain crystal symmetry axis plays a central role. Actually, Ikeda and Miyake have calculated that the hybridization gap Δ_k disappears at points on the zone boundary, giving rise to a nearly V-shaped DOS, in the case that the hybridization vanishes along the k_z axis.¹⁶ Remarkably, they have shown that a small DOS exists in the gaplike state even for a pure material and the impurity-induced DOS increases in proportion to the square root of impurity concentration as $N_{\text{res}}(E_F) \sim \sqrt{n_{\text{imp}}}$.

It was reported that the gapped state in CeNiSn and CeRhSb was sensitively affected by some impurities or imperfections from the previous work.¹⁸ It was shown from the transport and the thermal measurements that any type of alloying by 10% into either a Ni or Ce sublattice destroyed the energy gap.^{17–19} Accordingly, it is an important way to investigate the imperfection and/or the substitution effects of the pseudogap in CeNiSn by the NMR method.

In this paper we deal with the off-stoichiometric compound $\text{CeNi}_{1.01}\text{Sn}$ and the substituted compounds such as $\text{CeNi}_{1-x}\text{M}_x\text{Sn}$ ($M = \text{Co}$ and Cu) and $\text{Ce}_{1-x}\text{La}_x\text{NiSn}$. In the former, impurity scattering is a primary effect associated with the site disorder. A unique T dependence of $^{119}\text{(}1/T_1\text{)}$ allows us to deduce the characteristic change of the gap structure by the impurity scattering. We note that the substitution has two effects of doping carriers and acting as impurity scatterers. The replacement of $\text{Ni}(3d^8)$ by $\text{Co}(3d^7)$ or $\text{Cu}(3d^9)$ results in doping holes or electrons into the conduction band, respectively, since a photoemission study showed that the Ni $3d$ band is located close to the Fermi level and incompletely filled due to the hybridization with the unoccupied Sn $5p$ states.²⁰ As a result through the hybridization between $4f$ and conduction electrons, carriers are added into the quasiparticle bands. By contrast, the replacement of $\text{Ce}(4f^1)$ by $\text{La}(4f^0)$ is believed to add “Kondo holes” and destroy the coherence in the ground state.

This paper is organized as follows. In Sec II, we give a brief description of the experimental procedures. In Sec III, from the T dependence of the nuclear-spin lattice relaxation rate $^{119}\text{(}1/T_1\text{)}$ and the Knight shift ^{119}K , we address the change of the pseudogap structure in CeNiSn brought about by the presence of impurities or replacing Ce or Ni sites by other dopants. A summary is given in Sec IV.

II. EXPERIMENTAL DETAILS

Polycrystal and the single-crystal CeNiSn , off-stoichiometric $\text{CeNi}_{1.01}\text{Sn}$, and the substituted compounds such as $\text{CeNi}_{1-x}\text{M}_x\text{Sn}$ ($M = \text{Co}, \text{Cu}$) and $\text{Ce}_{1-x}\text{La}_x\text{NiSn}$ with $x = 0.01, 0.03, 0.06, 0.10$ were investigated by the ^{119}Sn NMR measurement. The detailed procedures for preparing polycrystals and single crystals were reported elsewhere.¹⁹ As reported in the previous work, the single crystals of

CeNiSn used here, which correspond to sample No. 4 in Ref. 9, were grown by the Czochralski method. The semiconducting behavior at low T was no longer observed in the T dependence of the resistivity. Importantly, it has, however, been confirmed from the present experiment that $1/T_1$ for single crystals undergoes almost the same T dependence as in the previous polycrystals down to the lowest temperature, although the resistivity behaves differently at low T . From this result, the bulk properties are expected to be affected by the presence of foreign phases, one of which was actually identified as CeNi₂Sn₂, or by microcracks, dislocations, lattice defects, etc., whereas the NMR result contrasts with the complication of the transport and the thermal properties. This may be because the Sn NMR is observed at different resonance fields for foreign phases like CeNi₂Sn₂ and the total fraction of Sn sites affected by such metallurgical imperfections is negligibly small. By contrast, the resistivity increases with lowering temperature because the presence of impurities and imperfections make carriers localized due to a small carrier density inherent to CeNiSn.

For the NMR measurement, all the samples were crushed into fine powder with diameter less than 70 μm to avoid the skin-depth effect of radio frequency fields. The ¹¹⁹Sn NMR experiment was carried out by using a laboratory-made phase-coherent pulsed NMR spectrometer at 20.7 and 3.5 MHz above and below 1.3 K, which corresponds to a magnetic field of about 12.7 and 2.2 kOe, respectively. In the NMR experiment at very low temperatures down to 0.015 K, it is necessary to avoid the eddy current heating up by radio frequency excitation pulses. So the NMR frequency was set as 3.5 MHz for the experiment below 1.3 K.¹⁰ Since the magnetic susceptibilities are highly anisotropic with the easy a axis, each grain is oriented along the easy a axis by giving mechanical vibrations in an external magnetic field. A narrow ¹¹⁹Sn NMR spectrum for the oriented powder was thus obtained with a full width of 20 Oe at half maximum. The spin-lattice relaxation time T_1 and Knight shift K of ¹¹⁹Sn were hence measured accurately.

$1/T_1$ did not depend on the magnetic field in the range of 2.2 kOe– (3.5 MHz–) 12.7 kOe (20.7 MHz) down to 1.3 K where $1/T_1$ experiences a large reduction due the opening of the gap. Furthermore, the specific heat and the magnetoresistance measured in smaller fields than 40 kOe does not indicate any change as compared to the zero-field data.^{21,22} Therefore we can safely ignore the magnetic field dependence of the gap in the present measurement. However, since a preliminary measurement of $1/T_1$ under a strong magnetic field of 80 kOe shows a significant suppression, it may be possible that the pseudogap identified by the NMR is depressed by such a strong enough field. The magnetic and the pressure dependences will be reported in a following paper.

III. EXPERIMENTAL RESULTS AND DISCUSSIONS

A. Spin-lattice relaxation rate of ¹¹⁹Sn, ¹¹⁹($1/T_1$)

1. Polycrystal and single-crystal CeNiSn

In CeNiSn, a crystal field scheme of the Ce³⁺ single ion is inadequate to describe the anisotropy of the susceptibility,

since well-defined crystal field splittings are not observed by the neutron scattering experiment due to the strong mixing (c - f mixing) effect between f and conduction electrons.²³ Even in the renormalized band picture, it is also possible that the g factors of quasiparticles near the Fermi level are strongly anisotropic due to the strong spin-orbit interaction. As far as the low-temperature properties are concerned below the characteristic temperature related to the c - f mixing energy, the band picture is applied to CeNiSn by incorporating a large anisotropy of the g factors.

In heavy electron systems one can observe indirectly fluctuations of f spins through the hybridization between f and conduction electrons. In general, one can write $1/T_1$ as

$$1/T_1 = 2\gamma^2 k_B T \sum_q (A_{-q} A_q) \frac{\text{Im}\chi_{\perp}(q, \omega_n)}{\omega_n}, \quad (3.1)$$

where $\text{Im}\chi_{\perp}(q, \omega_n)$ is a perpendicular component of the imaginary part of the dynamical susceptibility and $A_{-q}(A_q)$ and ω_n is the q -dependent transferred hyperfine coupling constant and the nuclear frequency, respectively. This general formula can be applied for both cases of metal and nonmetal.²⁴ In the case that the q dependence of spin fluctuations is not so large, with the use of

$$\sum_q \text{Im}\chi_{\perp}(q, \omega_n) = \pi \sum_{k, \sigma, k', \sigma'} \delta(E_{k, \sigma} - E_{k', \sigma'} - \hbar \omega_n) \times \{f(E_{k, \sigma}) - f(E_{k', \sigma'})\}$$

and of a single-particle spectral function or an effective DOS, $N_{\text{eff}}(E)$ for the renormalized quasiparticle band, the T dependence of $1/T_1$ is expressed as

$$1/T_1 \propto A_{\text{HF}}^2 T \int N_{\text{eff}}^2(E) \left\{ -\frac{\partial f(E)}{\partial E} \right\} dE, \quad (3.2)$$

where the q dependence of A_q is averaged over whole q space on the Fermi surface, $f(E)$ is the Fermi function, and $A_{\text{HF}}^2 = \gamma^2 \hbar^2 \langle A_{-q} A_q \rangle_{\text{av}}$. In a simple metal where the Fermi energy E_F is much larger than the temperature, being an order of 1 eV, and $N_{\text{eff}}(E)$ is almost independent of the energy around E_F ,

$$1/T_1 = \frac{\pi}{\hbar} A_{\text{HF}}^2 N^2(E_F) k_B T$$

is deduced where $N(E_F)$ is the DOS at the Fermi energy.²⁵ The T^3 -like dependence of $1/T_1$ of CeNiSn in a T range of 0.4–2 K reported previously was consistent with the model that the gapped state possesses a V-shaped structure near the Fermi level, i.e., $N_{\text{eff}}(E) \sim E$, as shown in Fig. 1(a). Subsequently, $1/T_1$ below 0.4 K was found to be proportional to the temperature as indicated by the open circle in Fig. 2, probing the presence of the finite DOS. Eventually, in order to interpret the overall relaxation behavior, we applied the model with the following DOS:

$$N_{\text{eff}}(E) = \frac{c}{(E - E_F)^2 + \left(\frac{D}{2}\right)^2} \quad \text{for } |E - E_F| > \Delta,$$

$$N_{\text{eff}}(E) = \frac{c}{(E - \Delta)^2 + \left(\frac{D}{2}\right)^2} \frac{|E - E_F|}{\Delta}$$

$$\text{for } |E - E_F| < \Delta - \delta,$$

$$N_{\text{eff}}(E) = \alpha \quad \text{for } |E - E_F| \leq \delta. \quad (3.3)$$

Such a *gapless* V-shaped DOS is schematically indicated in Fig. 1(b). Here Δ and δ are a half width of the V-shaped gap and an energy plateau, and $\alpha = N_{\text{res}}(E)/N_0(E)$, a fraction of the residual DOS, $N_{\text{res}}(E)$ to the normal DOS, N_0 , for a simple Lorentzian band without the gap, and c is a normalization constant so that $\int N_{\text{eff}}(E)dE = 1$.

The T dependence of $1/T_1$ for the single crystal, which undergoes no upturn of the resistivity at low T , is shown by a solid circle in Fig. 2 together with the previous data (open circles) for the polycrystalline sample. As seen clearly in the figure, both results are almost the same down to 40 mK, showing a $T_1 T = \text{const}$ behavior down to about 15 mK below 0.3 K for the single crystal. Both overall relaxation behaviors have been consistently explained by the *gapless* V-shaped model described above [see Fig. 1(b)] as indicated by the solid line in Fig. 2. From this fitting, we have estimated $\alpha \equiv N_{\text{res}}(E)/N_0(E) = 0.077$, the band width, $D = 140$ K, and the magnitude of the pseudogap, $\Delta = 14$ K.¹⁰ It is found that single-crystal CeNiSn possesses nearly the same amount of the residual DOS as in the previous polycrystalline sample. Such unique relaxation behaviors, that $1/T_1$ is suppressed over three orders of magnitude below 10 K and follows the $T_1 T = \text{const}$ law at very low T , are independent of whether

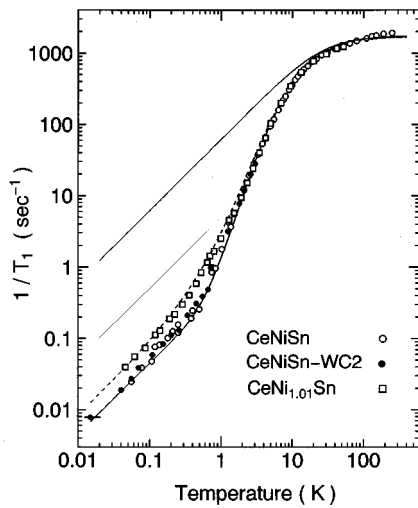


FIG. 2. T dependence of $1/T_1$ of ^{119}Sn in polycrystal (open circle) and single-crystal (solid circle) CeNiSn and CeNi_{1.01}Sn (open square). Solid and dashed lines are best fits based on the DOS in Figs. 1(b) and 1(c) for CeNiSn and CeNi_{1.01}Sn, respectively. Thin line is $T_1 T = \text{const}$ law calculated from the residual γ_{res} (see the text). The thick line is $T_1 T = \text{const}$ law for the quasiparticle band of Lorentzian shape without the V-shaped gap.

the resistivity increases or decreases with lowering temperature. The metallic behavior of the resistivity at low T , the $T_1 T = \text{const}$ law and the presence of the residual T -linear coefficient of the specific heat, γ_{res} , at very low T are strongly indicative of the presence of residual carriers at the Fermi level in CeNiSn. A fraction of the residual DOS, $\alpha(\gamma_{\text{res}}) = N_{\text{res}}(E)/N_0(E)$ is deduced from $\gamma_{\text{res}} \sim 40$ mJ/mol K² to be ~ 0.2 , which is considerably larger than $\alpha(\text{NMR}) = 0.077$. From the relation of $(T_1 T)_{\text{res}}^{-1}/(T_1 T)_0^{-1} = \alpha(\gamma_{\text{res}})^2$, where $(T_1 T)_0^{-1}$ without any gap is indicated by the thick solid line in Fig. 2, $(T_1 T)_{\text{res}}^{-1}$ is calculated as indicated by the thin solid line in Fig. 2. It should be noted that the amount of the residual DOS deduced from the T_1 data is smaller than that from the specific heat data involving all low-lying excitations.

2. Impurity effect in CeNi_{1.01}Sn

As indicated by an open square in Fig. 2, the T dependence of $1/T_1$ in the off-stoichiometric compound CeNi_{1.01}Sn is enhanced below 1 K as compared with the results for both polycrystal and the single-crystal CeNiSn. A larger value of $1/T_1 T$ at the low T regime is remarkable, pointing to the increase of the DOS for CeNi_{1.01}Sn. The model DOS shown in Fig. 1(b) does not reproduce the deviation from the T^3 behavior of $1/T_1$ below 1 K.²⁶ A careful analysis has revealed that agreement with the T_1 data has been obtained by the model DOS indicated not in Fig. 1(b), but in Fig. 1(c) where the flat DOS is absent *near* the Fermi level, but the DOS is enhanced *just at* the Fermi level. Namely, from a best-fitted curve indicated by the dashed line in Fig. 2, the same values of D and Δ and a larger $\alpha = 0.106$ are deduced for CeNi_{1.01}Sn. The impurity scattering introduced by the excess Ni atoms in CeNi_{1.01}Sn enhances the DOS *just at* the Fermi level and as a result obscures the flat DOS for the pure CeNiSn at the Fermi level associated with residual carriers.

3. Ce substitution: Ce_{1-x}La_xNiSn

To substitute La into Ce sites decreases the number of f electrons and the occupation of renormalized quasiparticle bands. Furthermore the nonmagnetic La impurities break the translational symmetry of the f sites and gradually the coherence of the ground state itself. The T dependences of $1/T_1$ in Ce_{1-x}La_xNiSn are indicated in Fig. 3 by an open triangle, solid circle, open square, and solid triangle for $x = 0.01, 0.03, 0.06,$ and 0.10 , respectively. It is remarkable that $1/T_1$ above 8 K does not depend on the La concentration x . By contrast, $1/T_1$ is strongly enhanced below 8 K with increasing x and in proportion to the temperature at low T . Interestingly, the data are well reproduced by the model DOS similar to Fig. 1(b) with the same parameters of $D = 140$ K and $\Delta = 14$ K as in pure CeNiSn, but a larger fraction of the residual DOS, $\alpha = 0.365, 0.576,$ and 0.749 for $x = 0.01, 0.03,$ and 0.06 , respectively. $1/T_1$ for $x = 0.10$ exhibits, however, a broad hump around 2.5 K, which cannot be reproduced by such the model DOS. Different from CeNi_{1.01}Sn where the DOS increases *at* the Fermi level, to dope La (Kondo holes) into Ce sites increases the flat DOS in a finite energy region near the Fermi level.

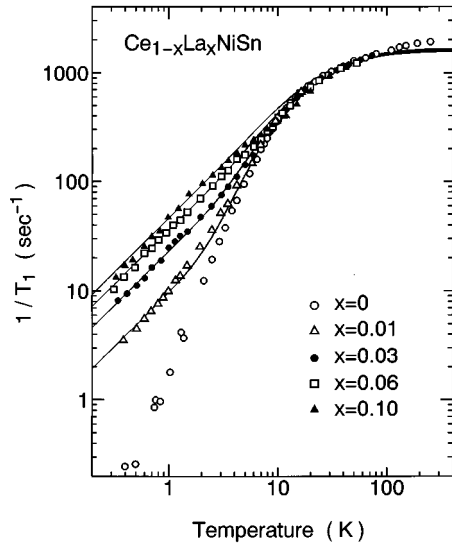


FIG. 3. T dependence of $1/T_1$ of ^{119}Sn in $\text{Ce}_{1-x}\text{La}_x\text{NiSn}$ ($x=0.01, 0.03, 0.06, 0.10$). Solid lines are best fits based on the DOS in Fig. 1(b).

4. Ni substitution: $\text{CeNi}_{1-x}\text{M}_x\text{Sn}$

a. $M = \text{Co}$. Substitution of Co into Ni sites decreases the number of d electrons in the conduction band. The T dependences of $1/T_1$ in $\text{CeNi}_{1-x}\text{Co}_x\text{Sn}$ are indicated by an open triangle, solid circle, open square, and solid triangle for $x=0.01, 0.03, 0.06$, and 0.10 in Fig. 4, respectively. $1/T_1$ is largely enhanced below 8 K with increasing Co content. For $x=0.03$, the T^3 dependence disappears and the $T_1T = \text{const}$ behavior holds down to 40 mK. $1/T_1$ for $x=0.10$ starts to deviate downward as compared with that of $x=0$ below 25 K and show a $T_1T = \text{const}$ behavior below 10 K. A systematic T variation of $1/T_1$ is well fitted based on the same model applied to the La substituted systems [Fig. 1(b)] as indicated by the solid line in Fig. 4. Without any appreciable change of

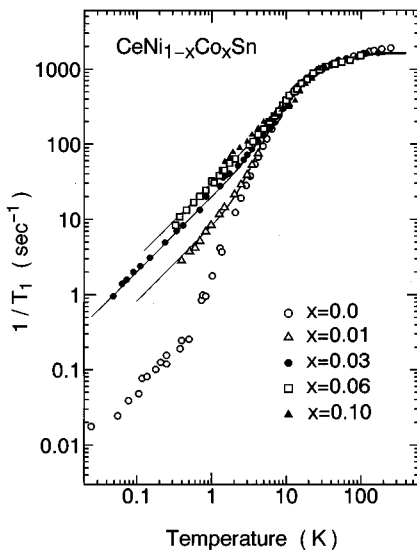


FIG. 4. T dependence of $1/T_1$ of ^{119}Sn in $\text{CeNi}_{1-x}\text{Co}_x\text{Sn}$ ($x=0.01, 0.03, 0.06, 0.10$). Solid lines are best fits based on the DOS in Fig. 1(b).

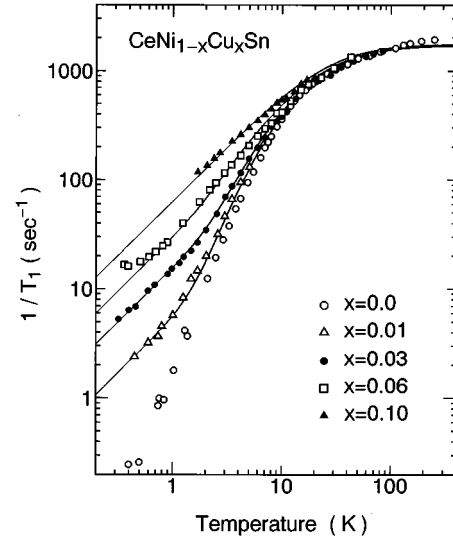


FIG. 5. T dependence of $1/T_1$ of ^{119}Sn in $\text{CeNi}_{1-x}\text{Cu}_x\text{Sn}$ ($x=0.01, 0.03, 0.06, 0.10$). Solid lines are best fits based on the DOS in Fig. 1(b).

$\Delta = 14$ K, the progressive increase of the fraction of the DOS, α , is obtained to be 0.336, 0.528, and 0.672 for $x=0.01, 0.03$, and 0.06 , respectively. Remarkably, the effect to fill up the V-shaped gap by replacing Ni by Co is almost the same as that by replacing Ce by La. For both cases, the flat DOS increases near the Fermi level with increasing La and Co content. By contrast, the DOS just at the Fermi level increases in $\text{CeNi}_{1.01}\text{Sn}$ as mentioned above. This suggests that La and Co atoms not only act as impurity scatterers, but also work as hole suppliers into the coherent band formed by the hybridization between f and conduction electrons.

b. $M = \text{Cu}$. Contrary to the La or the Co substitution, the Cu substitution increases the number of d electrons in the conduction band. The T dependences of $1/T_1$ for $\text{CeNi}_{1-x}\text{Cu}_x\text{Sn}$ with $x=0.01, 0.03, 0.06$, and 0.10 are shown in Fig. 5, respectively. It is notable for the Cu substitution that the T dependence of $1/T_1$ deviates from that in CeNiSn below 30 K which is considerably higher than below 8 K for the La and the Co substitution. For $x=0.01$ and 0.03 , the $T_1T = \text{const}$ behavior is valid below 1 K,²⁷ whereas for $x=0.06$, a $T_1T = \text{const}$ behavior is no longer observed below 0.5 K and, furthermore, as indicated in Fig. 6, the full width at half maximum of the NMR spectrum begins to broaden progressively below 1.3 K, whereas that for the La substitution stays constant. For $x=0.10$, the NMR spectrum is largely wiped out below 1.3 K, which prevents us from measuring $1/T_1$. Such a broadening of the NMR spectrum provides a signature of an AF ordering. As a matter of fact, it was reported that the AF ordering takes place at $T_N \approx 2.6$ K for $x=0.13$ from the magnetic susceptibility measurement.¹⁹

Since we failed to apply the V-shaped model with the flat DOS as in Fig. 1(b) for the Cu substitution, we have tried to make the magnitude of the gap (Δ) reduce with increasing Cu content, keeping $D=140$ K constant. The solid line in Fig. 5 indicates a best fit with Δ to be 12, 11, 7, and 0 K for $x=0.01, 0.03, 0.06$, and 0.10 and $\alpha=0.269, 0.461$, and 0.653 for $x=0.01, 0.03$, and 0.06 , respectively. Remarkably, the

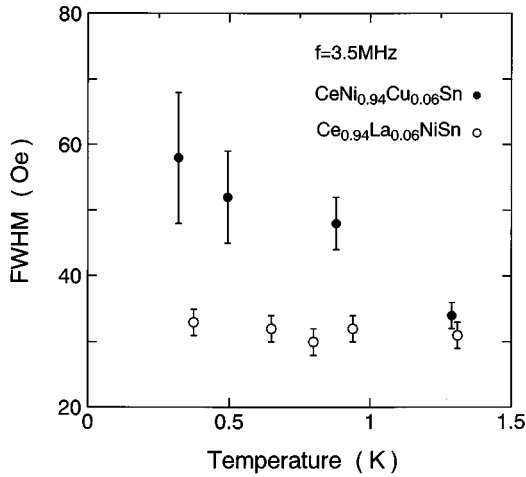


FIG. 6. T dependence of the full width at half maximum (FWHM) in Cu and La substituted CeNiSn for $x=0.06$. A significant increase of the FWHM for Cu substitution gives evidence for the onset of AF order. In Cu substituted compounds with $x=0.1$, the Sn NMR spectrum is wiped out below 1.5 K.

effect to fill up the V-shaped gap by replacing Ni by Cu is more substantial than for the La and the Co substitution. The Cu substitution induces not only the DOS, but also reduces the magnitude of the energy gap. This suggests that to dope electrons by the Cu substitution suppresses more markedly the gapped state than to dope holes by either the La or the Co substitution does.

Figure 7 shows the concentration(x) dependence of relative fraction of the DOS, $\alpha = [N_{\text{res}}(E)/N_0(E)]$, estimated from the value of $1/T_1T$ for $x < 0.10$. Independent of the dopant, all the data are fitted by the formula of $[N_{\text{res}}(E)/N_0(E)] = A\sqrt{x} + 0.077$. Solid, short-dashed, and long-dashed lines are the fits with $A = 2.27, 2.49$, and 2.80 for the Cu, the Co, and the La substituted systems, respectively. On the other hand, the \sqrt{x} dependence of γ_{res} has been observed in $(\text{Ce}_{1-x}\text{La}_x)_3\text{Bi}_4\text{Pt}_3$, whereas γ_{res} increases

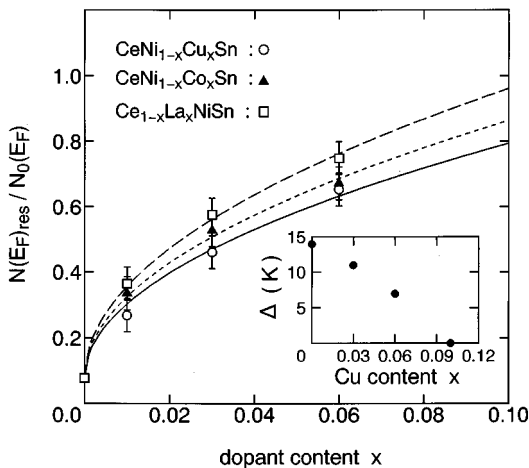


FIG. 7. Dopant dependences of the flat DOS at the Fermi level. Solid, short-dashed, and long-dashed lines are least squares fits to the data for Cu, Co, and La substituted systems, respectively. The inset shows the dependence of the gap value on x in $\text{CeNi}_{1-x}\text{Cu}_x\text{Sn}$.

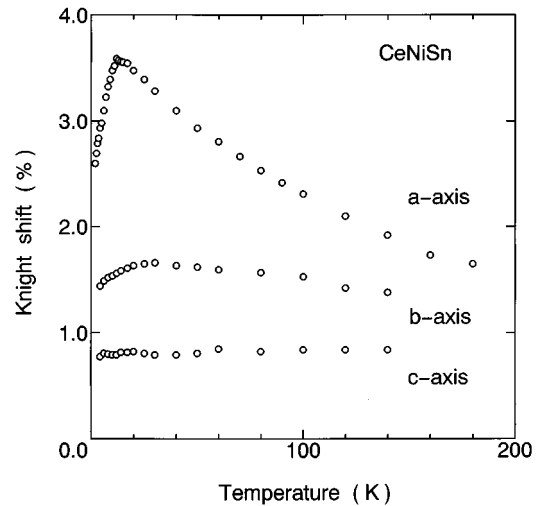


FIG. 8. T dependence of the ^{119}Sn Knight shift of CeNiSn along a, b, c axes. (Ref. 10).

in proportion to x in ligand-substituted systems, $\text{Ce}_3\text{Bi}_4(\text{Pt}_{1-x}\text{Au}_x)_3$.²⁸ From theoretical points of view, the \sqrt{x} dependence of the DOS was argued from a general context of the doping effect in Kondo insulator by Schlottmann¹⁵ and from a different context in CeNiSn and CeRhSb by Ikeda and Miyake.¹⁶ In the former, for a finite content of Kondo holes by the La substitution, the f -derived DOS of the impurity band is proportional to \sqrt{x} at the Fermi level, whereas for ligand impurities such as Co and Cu, the tails of impurity states develop close to the gap edge. The latter has shown that even for pure CeNiSn a small DOS exists in the pseudogap state caused by the highly anisotropic hybridization and, furthermore, the induced DOS increases in proportion to \sqrt{x} . In CeNiSn, a primary cause to suppress the V-shaped gap is not due to the impurity scattering, but to the increase of carrier density by the substitution, because the impurity scattering as shown in $\text{CeNi}_{1.01}\text{Sn}$ gives rise to only a small amount of the residual DOS at the Fermi level.

B. ^{119}Sn Knight shift

In order to confirm a validity of the V-shaped model of the gap structure in the undoped CeNiSn, the T dependence of the Knight shift has been measured. As reported previously, the magnetic susceptibility of CeNiSn shows a Curie tail at low T , whereas the Knight shifts parallel to a , b , and c axes reflect the intrinsic susceptibility of CeNiSn without any influence by a small amount of magnetic impurities. Figure 8 shows the highly anisotropic T dependence of the ^{119}Sn Knight shift. The Knight shift along the a axis undergoes a rapid drop below 12 K associated with the opening of the gap. By contrast, the shift along the c axis stays constant, dominated by the Van Vleck contribution.¹⁰

In general, the Knight shift for ligand sites in $4f$ compounds is dominated by the T dependent spin part $K_s(T)$ and the T -independent Van Vleck part K_{VV} as

$$K(T) = K_s(T) + K_{\text{VV}}. \quad (3.4)$$

Here, the contribution from conduction electrons is negligible. Concomitantly, the magnetic susceptibility has two

contributions of the spin part $\chi_s(T)$ and the Van Vleck part χ_{VV} as

$$\chi(T) = \chi_s(T) + \chi_{VV}. \quad (3.5)$$

The spin Knight shift of ^{119}Sn , $K_s(T)$, is dominated by the f -derived susceptibility through the transferred hyperfine interaction originated from the hybridization between f electrons at Ce sites and s or p electrons at Sn sites. $K_s(T)$ is related to $\chi_s(T)$ by the transferred hyperfine coupling constant A_{HF} as follows:

$$K_s(T) = \frac{A_{\text{HF}}}{N_A \mu_B} \chi_s(T), \quad (3.6)$$

where N_A and μ_B are Avogadro's number and the Bohr magneton, respectively. Based on the quasiparticle band picture, $\chi_s(T)$ is evaluated as follows:

$$\chi_{s,i}(T) \propto g_i \mu_B \int N_{\text{eff}}(E) \left\{ -\frac{\partial f(E)}{\partial E} \right\} dE, \quad (3.7)$$

where i denotes the crystal direction and $N_{\text{eff}}(E)$ the effective DOS defined by (3.3). The anisotropy originates from that of the g factors. As seen in Fig. 8, the Knight shifts remain finite at $T=0$ along all crystal directions. The spin and the Van Vleck contributions are difficult to separate, because the f -derived moment induced by the magnetic field contributes to the spin shift with increasing temperature. If K_{VV} along the a axis at low T is assumed to be nearly the same as $K_c=0.8\%$ dominated by K_{VV} (see Fig. 8), the spin Knight shift $K_{s,a}(T)$ along the a axis is roughly estimated as indicated in Fig. 9. From (3.3) and (3.7), the relative T dependence of the spin Knight shift is calculated with the parameters of $D=140$ K, $\Delta=14$ K, and $\alpha=0.077$ as indicated by dashed line in Fig. 9. In a T range higher than the temperature 12 K at the peak of the shift, the agreement seems to be satisfactory, but the decrease of the shift below 12 K is not reproduced. Rather a better fit is obtained with a different set of parameters of $D=200$ K, $\Delta=5$ K, and $\alpha=0.451$ as indicated by the solid line.

Apparently, the T dependence of $1/T_1$ and the spin Knight shift are not consistently reproduced with the same effective DOS. Therefore an estimation of $K_{VV}=0.8\%$ along the a axis comes into question because K_{VV} might be highly anisotropic. Such an ambiguity for the estimation of K_{VV} makes it difficult to extract the gap structure from the Knight shift data with the same accuracy as from the T_1 data.

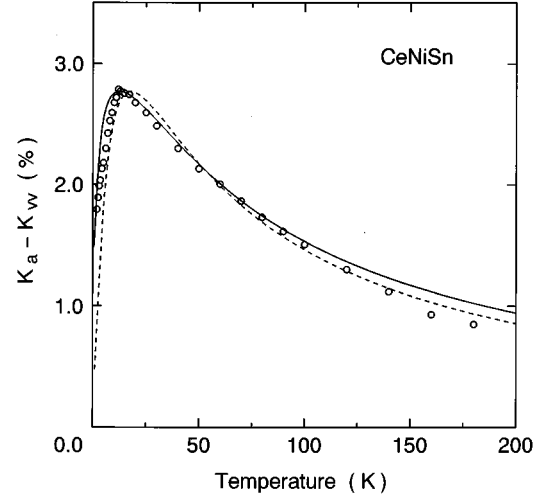


FIG. 9. T dependence of the ^{119}Sn spin Knight shift of CeNiSn along the a axis, where $K_{VV}=0.8\%$ is assumed to be the same as for the c axis. Solid and dashed lines are calculations based on the model DOS in Fig. 1(b) with $D=200$ K, $\Delta=5$ K, and $\alpha=0.451$ and with $D=140$ K, $\Delta=14$ K, and $\alpha=0.077$, respectively.

IV. SUMMARY

From systematic NMR experiments on single-crystal CeNiSn and the substituted systems, it has been deduced that the intrinsic DOS at the Fermi level exists even in the better single-crystal CeNiSn, which should be hence classified as the semimetal with very low carrier density. It has been clarified that the DOS inside the V-shaped pseudogap is induced just at the Fermi level by adding impurities as in the off-stoichiometric compound CeNi_{1.01}Sn, whereas the flat DOS is induced over a finite energy range near the Fermi level by substituting La and Co into Ce and Ni sites, respectively. Furthermore, the La and the Co substitution do not change the magnitude of the energy gap with $\Delta=14$ K, whereas the Cu substitution reduces the gap in addition to the increase of the DOS. In the latter case, AF ordering takes place for the Cu substitution with more than $x=0.06$. Namely, depending on whether holes or electrons are doped into the renormalized conduction bands, the V-shaped gapped state changes into either a normal Fermi liquid state or the antiferromagnetic ground state.

ACKNOWLEDGMENTS

We gratefully acknowledge Professor K. Miyake and H. Ikeda for valuable comments. This work was supported by the Grant-in-Aid for Scientific Research from the Ministry of Education, Science and Culture of Japan.

- ¹A. Jayaraman, V. Narayanamurti, E. Bucher, and R.G. Maines, Phys. Rev. Lett. **25**, 1430 (1970); M. Takigawa, H. Yasuoka, Y. Kitaoka, T. Tanaka, H. Nozaki, and Y. Ishizawa, J. Phys. Soc. Jpn. **50**, 2525 (1981).
- ²M. Kasaya, F. Iga, M. Takigawa, and T. Kasuya, J. Magn. Magn. Mater. **47&48**, 429 (1985).
- ³P. Wachter and G. Travaglini, J. Magn. Magn. Mater. **47&48**, 423 (1985).

- ⁴J. Flouquet, P. Haen, and C. Vettier, J. Magn. Magn. Mater. **29**, 159 (1982).
- ⁵P.A. Alekseev, J.-M. Mignot, J. Rossat-Mignot, V.N. Lazukov, and I.P. Sadikov, Physica B **186-188**, 384 (1993).
- ⁶T. Takabatake, Y. Nakazawa, and M. Ishikawa, Jpn. J. Appl. Phys. Suppl. **26**, 547 (1987); T. Takabatake, F. Teshima, H. Fujii, S. Nishigori, T. Suzuki, T. Fujita, Y. Yamaguchi, J. Sakurai, and D. Jaccard, Phys. Rev. B **41**, 9607 (1990).

- ⁷S.K. Malik and D.T. Adroja, *Phys. Rev. B* **43**, 6277 (1991).
- ⁸M.F. Hundley, P.C. Canfield, J.D. Thompson, and Z. Fisk, *Phys. Rev. B* **42**, 6842 (1990).
- ⁹G. Nakamoto, T. Takabatake, Y. Bando, H. Fujii, K. Izawa, T. Suzuki, T. Fujita, A. Minami, I. Oguro, L.T. Tai, and A.A. Menovsky, *Physica B* **206&207**, 840 (1995).
- ¹⁰M. Kyogaku, Y. Kitaoka, H. Nakamura, K. Asayama, T. Takabatake, F. Teshima, and H. Fujii, *J. Phys. Soc. Jpn.* **59**, 1728 (1990).
- ¹¹K. Nakamura, Y. Kitaoka, K. Asayama, T. Takabatake, H. Tanaka, and H. Fujii, *J. Phys. Soc. Jpn.* **63**, 433 (1994).
- ¹²A.P. Reyes, R.H. Heffner, P.C. Canfield, J.D. Thompson, and Z. Fisk, *Phys. Rev. B* **49**, 16 321 (1994).
- ¹³T.E. Mason, G. Aeppli, A.P. Ramirez, K.N. Clousen, C. Broholm, N. Stücheli, E. Bucher, and T.T.M. Palstra, *Phys. Rev. Lett.* **69**, 490 (1992).
- ¹⁴H. Kadowaki, T. Sato, H. Yoshizawa, T. Ekino, T. Takabatake, H. Fujii, L.P. Regnault, and Y. Ishikawa, *J. Phys. Soc. Jpn.* **63**, 2074 (1994); T.J. Sato, H. Kadowaki, H. Yoshizawa, T. Ekino, T. Takabatake, H. Fujii, L.P. Regnault, and Y. Ishikawa, *J. Phys. Condens. Matter* (to be published).
- ¹⁵P. Schlottman, *J. Appl. Phys.* **75**, 7044 (1994).
- ¹⁶H. Ikeda and K. Miyake, *J. Phys. Soc. Jpn.* (to be published).
- ¹⁷F.G. Aliev, *Physica B* **171**, 199 (1991).
- ¹⁸T. Takabatake, G. Nakamoto, H. Tanaka, H. Fujii, S. Nishigori, T. Suzuki, T. Fujita, M. Ishikawa, I. Oguro, M. Kurisu, and A.A. Menovsky, in *Transport and Thermal Properties of f-Electron Systems*, edited by G. Oomi *et al.* (Plenum Press, New York, 1993), p. 1.
- ¹⁹T. Takabatake, Y. Nakazawa, M. Ishikawa, T. Sakakibara, K. Koga, and I. Oguro, *J. Magn. Magn. Mater.* **76&77**, 87 (1988).
- ²⁰S. Nohara, H. Namatame, A. Fujimori, and T. Takabatake, *Physica B* **186-188**, 403 (1993); S. Nohara, H. Namatame, and T. Takabatake, *Phys. Rev. B* **47**, 1754 (1993).
- ²¹T. Takabatake, M. Nagasawa, H. Fujii, G. Kido, M. Nohara, S. Nishigori, T. Suzuki, and T. Fujita, *Phys. Rev. B* **45**, 5740 (1992).
- ²²K. Sugiyama, T. Inoue, K. Oda, T. Takabatake, H. Tanaka, H. Fujii, G. Kido, and M. Date, *Physica B* **211**, 223 (1995).
- ²³M. Kohgi, K. Ohoyama, T. Osakabe, and M. Kasaya, *J. Magn. Magn. Mater.* **108**, 187 (1992).
- ²⁴T. Moriya, *J. Phys. Soc. Jpn.* **18**, 516 (1963).
- ²⁵J. Korryng, *Physica* **16**, 601 (1950).
- ²⁶K. Nakamura, Y. Kitaoka, K. Asayama, T. Takabatake, G. Nakamoto, H. Tanaka, and H. Fujii, *Physica B* **206&207**, 829 (1995).
- ²⁷Y. Kitaoka, M. Kyogaku, K. Nakamura, G.-q. Zheng, H. Nakamura, K. Asayama, T. Takabatake, H. Tanaka, H. Fujii, and T. Suzuki, *Physica B* **186-188**, 431 (1993).
- ²⁸J.D. Thompson, W.P. Beyermann, P.C. Canfield, Z. Fisk, M.F. Hundley, G.H. Kwei, R.S. Kwok, A. Lacerda, J.M. Lawrence, and A. Severing, in *Transport and Thermal Properties of f-Electron Systems*, edited by G. Oomi *et al.* (Plenum Press, New York, 1993), p. 35.